TU Delft

Delft University of Technology

Healing of a glass fibre reinforced composite with a disulphide containing organic-inorganic epoxy matrix

Post, W.; Cohades, A.; Michaud, V; van der Zwaag, S.; Garcia, S. J.

DOI
10.1016/j.compscitech.2017.09.017

Publication date
2017

Document Version
Accepted author manuscript

Published in
Composites Science and Technology

Citation (APA)
Post, W., Cohades, A., Michaud, V., van der Zwaag, S., & Garcia, S. J. (2017). Healing of a glass fibre reinforced composite with a disulphide containing organic-inorganic epoxy matrix. *Composites Science and Technology*, *152*, 85-93. https://doi.org/10.1016/j.compscitech.2017.09.017

Important note
To cite this publication, please use the final published version (if applicable).
Please check the document version above.

Copyright
Other than for strictly personal use, it is not permitted to download, forward or distribute the text or part of it, without the consent of the author(s) and/or copyright holder(s), unless the work is under an open content license such as Creative Commons.

Takedown policy
Please contact us and provide details if you believe this document breaches copyrights.
We will remove access to the work immediately and investigate your claim.

This work is downloaded from Delft University of Technology.
For technical reasons the number of authors shown on this cover page is limited to a maximum of 10.

Healing of a glass fibre reinforced composite with a disulphide containing organic-inorganic epoxy matrix

W. Post[1], A.M. Cohades[2], V. Michaud[2], S. van der Zwaag[1], S. J. García[1*]

[1]*Novel Aerospace Materials Group, Faculty of Aerospace Engineering, Technical University of Delft, Kluyverweg 1, 2629 HS, Delft, The Netherlands*

[2]*Laboratory for Processing of Advanced Composites (LPAC), Ecole Polytechnique Fédérale de Lausanne (EPFL), Station 12, CH-1015 Lausanne, Switzerland*

Keywords: Functional composites, self-healing, fracture toughness, impact behaviour, thermomechanical properties

Abstract

We report the development of an intrinsic healing glass fibre reinforced polymer (GFRP) composite based on a disulphide-containing organic-inorganic thermoset matrix. Thermomechanical experiments showed that the newly developed matrix has a unique combination of Young's modulus (800-1200 MPa), multiple thermally induced healing (70-85°C), and processability by conventional vacuum infusion process. The composite mechanical properties and the extent of healing were determined by flexural, fracture and low-velocity impact testing. Small sized (<cm^2) damage could be partially healed multiple times using a minimal healing pressure to ensure a good alignment of the damaged interfaces. The level of healing can be enhanced, even for large (>cm^2) damage, by increasing the healing pressure provided the location of the primary damage is concentrated within the matrix phase. The polymer matrix composite introduced here represents a significant step forward from the often mechanically inferior intrinsically self-healing composites towards structural self-healing composites.

1. Introduction

Over the past decades, fibre reinforced polymer composites (FRPCs) have found their way into numerous lightweight structural, automotive and aerospace applications. However, their complex failure behaviour and high susceptibility to impact and fatigue damage makes FRPCs hard to repair after being damaged. As such, it is of high interest to develop FRPCs that can heal themselves multiple times, thereby extending their overall lifetime [1-3]. Thermoset polymer matrices (i.e. polymers having a decent dimensional stability under load) with an intrinsic healing ability (i.e. the healing stems from the polymer architecture itself) are considered to be ideal candidates for the recovery of frequently occurring damage modes in fibre reinforced polymer composites, such as barely visible impact damage, matrix cracking and delaminations [4-6]. Contrary to approaches based on extrinsic self-healing polymeric systems (i.e. polymers with embedded discrete healing agents capable of healing e.g. flexural [7,8], fracture [9,10] and impact damage [11,12]), composites based on intrinsic healing polymers can undergo multiple healing events provided the damage to the reinforcing fibres is not excessive or highly localised [13]. Over the past decade several polymer matrices, with proven intrinsic healing capacity, have been proposed for polymer composites. The most common approach is by using matrices containing reversible Diels Alder moieties which have a high compatibility with conventional epoxy matrices [14-16]. Another approach is the use of thermoplastic ionomers, which are of interest due to their relatively high thermomechanical properties during healing [17-19]. Recently, glass fibre composites were manufactured with the supramolecular polymer Reverlink (from Arkema) which showed healing at room temperature [20]. Another common strategy is the blending of immiscible thermoplastic polymers with epoxy-based thermosets. Upon melting, the thermoplastic phase flows into the damaged region while the thermoset phase ensures the mechanical stability [21-23]. However, all these examples result in composites, which are also marked by either low mechanical properties, high (>100°C) healing temperatures, unconventional manufacturing routes or a combination of these undesirable factors.

A promising recent approach to obtain a good combination of adequate mechanical properties and healing at low temperature is the introduction of covalently bonded disulphide groups within a conventional epoxy based network. These systems, which were initially reported by Sastri and Tesoro [24,25], combine mild healing temperatures (<100°C) with relatively high mechanical properties (Young's modulus within the range of 20-200 MPa) and proved to be ideal candidates for the development of self-healing coatings [26-28], rubbers [29] and composites [30,31]. However, the majority of these polymer systems still have insufficient mechanical properties and their complex chemistries (resulting in high viscosities or fast reactivity) make conventional composite processing impractical for application in structural composites. Additionally, these polymers often require a healing temperature that is similar to or even higher than their curing temperature. For example, Odriozola et al. developed FRPCs, cured at 150°C, with mechanical properties similar to commercial epoxy composites while the selected repair temperature is 200°C [31]. As a result, it is difficult to decouple healing and post-curing effects. Furthermore the overlap of healing and curing temperatures will ultimately limit the possibility of multiple healing. In addition, it has to be noted that the typical disulphide containing monomers (dithioamines) used for the synthesis of the polymers are very expensive compared to commercial epoxy monomers. In intrinsic healing of polymeric matrices, a high elastic modulus (at room temperature) is generally accompanied by a high healing temperature. Figure 1 summarizes the major developments in the field by representing the elastic modulus versus the healing temperature of a wide range of intrinsic healing polymer matrices. The figure includes branched polyetherimide (PEI) elastomers [32], multiphase elastomers [33], supramolecular elastomers [34-36], human skin [37], disulfide based elastomers [29], metallopolymers [38], ionomers and ionomer blends [19,39], Diels-Alder based polymers [40,41], epoxy-PCL blends [21], vitrimers [42,43] and the family of disulfide based epoxy thermosets [28,30]. For comparison, a selection of engineering thermoplastics at their melting temperatures was added to the figure [44]. Figure 1 clearly shows that the current challenge in self-healing polymers lies within the development of systems with a

high modulus and low healing temperature in order to reach properties of interest that can compete with commerical high performance polymers.

Figure 1 shows that the disulphide based thermosets are among the polymer systems closest to the target region for intrinsic self-healing polymers, thereby indicating that these polymers are a good starting point for the development of self-healing fibre composites with good mechanical properties. This work presents a next step in this direction by introducing a self-healing glass fibre reinforced polymer (GFRP) composite based on an organic-inorganic disulphide containing epoxy thermoset. This polymeric system shows multiple healing upon a short thermal treatment of 70°C and has mechanical properties (20-200 MPa) suitable for coating applications [28,45]. Furthermore, the sulphide containing monomers are less expensive compared to those of other disulphide containing thermosets [24,25,31]. To allow for processing by conventional composite manufacturing routes the polymer matrix curing kinetics were slowed down by modifying the polymer composition. The effect of the curing conditions on the room temperature stiffness and the matrix network mobility at elevated temperatures was investigated. Subsequently, GFRPs were prepared and their multiple healing capabilities at modest temperatures were evaluated by conventional flexural, fracture and low-velocity impact testing.

2. Experimental

2.1. Materials

Epon ^{TM} 828 resin was purchased from Momentive. Ancamine®2500 curing agent was purchased from Air Products. (3-Aminopropyl)trimethoxysilane (97%), Pentaerythritol tetrakis(3-mercaptopropionate) and Triethylamine from hereon called APTS, tetrathiol and TEA respectively, were purchased from Sigma–Aldrich. Bis[3-(triethoxysilyl)propyl]disulfide (99%), from hereon called BDS, was purchased from Capture Chemicals. All chemicals were used as received without further purification. The selected glass fibre reinforcement was a woven twill 2 × 2 E-glass fabric, with a nominal areal weight of 390 g.m^{-2} , 6 end cm^{-1} for warp fibres and 6.7

picks cm^{-1} for weft fibres, fibre diameter of 9 μm yarn thickness of 0.45 mm, warp tex of 68 × 5 and weft tex of 272, from Suter-Kunststoffe AG.

2.2. Resin and GFRPs production

2.2.1. Resin preparation

The selected polymer matrix is an adaptation of a dual network polymer network reported in previous studies [28,30] and is composed of six different components. Compared to this previous work Bis[3-(triethoxysilyl)propyl]tetrasulfide (BTS) was replaced by BDS. To facilitate the disulphide cleavage essential in matrix healing TEA was added as a catalyst.

Epon ™ 828, APTS and BDS were pre-stirred using a magnetic stirrer for 3 hours at room temperature. Ancamine® 2500 was then added and the mixture was manually stirred for 3 minutes until the mixture was fully homogeneous. The resulting mixture and the tetrathiol were then degassed in a vacuum chamber for 10 minutes. Then, TEA and tetrathiol were added and the final resin was manually stirred for another 5 minutes. The weight ratio of all resin components is depicted in Table I. For characterization of the free standing polymer matrix, the resin was poured into a Teflon mould and was cured for 24 hours at room temperature followed by 60 hours curing at 100°C under ambient conditions.

2.2.2. Composite processing

A total of 600 gram of resin was prepared per composite plate. In order to increase the pot-life, this amount was divided into two batches of 300 gram resin each. The resin viscosity was found to be below 0.5 Pa.s at room temperature (determined by a rheometer AR 2000 from TA Instruments). The resin was therefore infused at room temperature into a stack of 20 x 30 cm glass fibre reinforcement layers with a $[(+45/–45)/(0/90)]_{4s}$ sequence using conventional vacuum assisted resin infusion moulding (VARIM) as described in previous work [20]. To improve the resin impregnation an additional flow mesh was placed at the bottom of the product. Following this procedure a plate thickness of 4.5 mm and a fibre volume fraction of 50 vol.% were targeted.

A Teflon film (Cytec, 15 μm, non-perforated) was inserted in between the two central plies to form the notch in the specimens that were prepared for double cantilever beam testing. After infusion the resulting product was first cured for 24 hours at room temperature under vacuum conditions and then for 60 hours at 100°C under ambient conditions. After this final curing step the composite plates were cooled down and cut with a diamond saw to obtain the preferred test specimen geometries.

2.3. Characterization methods

2.3.1. Matrix characterization

The effect of different curing treatments on the properties of the matrix polymer was investigated with thermal and mechanical testing techniques. The thermo-mechanical properties were measured by dynamic mechanical analysis (DMA) using a TA Instruments DMA Q800 operating in single cantilever bending mode. Rectangular specimens (35 x 12.5 x 2 mm) were heated from -50°C to 150°C with a heating ramp of 5°C/min. A frequency of 1 Hz and a strain of 0.02% were applied. The tensile behaviour of the matrix was investigated according to ASTM D1708-13 using an Instron Model 3365 universal testing systems equipped with a 1 kN load cell. Dog-bone micro-tensile specimens were loaded until failure at 2 mm/min at room temperature. A total number of 5 samples were tested per test condition.

2.3.2. GFRP composite characterization

Three methods of mechanical characterization were selected to investigate the properties of the composites and their self-healing behaviour: 3-point bending, double cantilever beam (DCB) and low-velocity impact testing.

3-point bending experiments were performed according to ASTM D790 to determine the healing of the flexural properties of the composites. A UTM Series LFM-125kN (Walter and Bai), equipped with a 10 kN load cell, was used in compression mode. Specimens were 220 mm long, 15 mm wide and approximately 4.5 mm thick. 1 test condition (85°C healing at 0.2 bar) was

repeated 5 times, the remaining test conditions were only performed once. A span-to-depth ratio of 40:1 was used and a crosshead speed of 2 mm/min was applied. As the specimen did not fully fracture, the experiment was terminated after a maximum centre beam deflection of 25 mm was obtained. The flexural stress was calculated using equation (1) [46]:

$$\sigma_f = \left(\frac{3PL}{2bd^2}\right)\left[1 + 6\left(\frac{D}{L}\right)^2 - 4\left(\frac{d}{L}\right)\left(\frac{D}{L}\right)\right] \quad (1)$$

where σ_f is the flexural stress (MPa), L is the support span (mm), d is the depth of beam (mm), P is the measured load at a given point (N), b is the beam thickness (mm), and D is the deflection of the centerline of the specimen at the middle of the support span (mm). The flexural strain was calculated using equation (2) [46]:

$$\varepsilon_f = \frac{6Dd}{L^2} * 100 \quad (2)$$

where ε_f is the flexural strain (%). The flexural modulus was calculated using [46]:

$$E_B = \frac{L^3 m}{4bd^3} \quad (3)$$

Where E_B is the flexural modulus (MPa) and m is the slope of the linear section of the load-deflection curve between 0 and 0.05 % strain (N/mm). The extent of damage and healing after the 3-point bending experiments was visualized using a digital microscope Keyence VHX2000 with a wide-range zoom lens (100x-1000x magnification). For the optimal illumination of the surfaces the microscope was equipped with a OP-87229 short ring-light.

Mode I opening of DCB specimens was performed following ASTM D5528. A Zwick mechanical testing machine (model 1455) equipped with a 20 kN load cell was used. A constant crosshead speed of 5 mm/min was applied and the experiment was stopped when a final displacement of 50 mm was achieved. The crack growth was monitored by a camera that was positioned perpendicular to the crack progression. Using the modified beam theory the local fracture toughness (G_I) was determined using [47]:

$$G_I = \frac{3P\delta}{2b(a + |\Delta|)} \quad (5)$$

Where δ is the load-point displacement (mm), a is the delamination length (mm) and |Δ| is the experimental correction factor which is determined by generating a least squares plot of the cube root of the compliance as a function of the delamination length, as is described by ASTM D5528. One sample was tested per test condition.

Low-velocity impact tests were performed according to ASTM D7136 using a free fall impact tower (Rosand IFW) with a 5.5 kg mass and 16 mm diameter hemispherical aluminium impactor. Samples of 80 x 80 mm were used. Three samples were tested per test condition. Samples were impacted with relatively low impact energies of 8, 16 or 30 Joule in order to mainly induce delamination and to minimize fibre breakage. A 60 kN Kistler load cell was used to measure the impact force and light gages were used to measure the inbound and rebound speed of the impactor. The level of dissipated energy (E_d) per impact condition was determined by [48]:

$$E_d = \frac{1}{2} m(v_{in} - v_{out})^2 \quad (6)$$

Where m is the mass of the impactor (kg) and v_{in} and v_{out} are the inbound and rebound speed (m/s) respectively. The extent of damage was monitored by taking photographs before and after healing. The photographs before and after healing were further processed using a Matlab code and binarized with a threshold of 0.125 in order to estimate the healed areas per impact energy.

2.3.3. Healing treatment

Healing of specimens subjected to bending and impact was performed at room temperature (RT), 70, 85 and 100°C using a hot-air furnace for 16 hours. Contact between the damaged interfaces during healing was ensured by dead weight loading at a constant pressure of 0.2 bar. The specimens tested by Mode I opening were healed at 85°C and 0.2, 2.0 and 20 bar whereby the higher pressure conditions (2.0 and 20 bar) were applied using a hot-press. The thickness of the composites was not affected by the applied healing treatments. The effect of healing time is

beyond the scope of this study, but a justification of using a relatively long healing time of 16 hours is given in Supplementary Information S4.

3. Results & discussion

3.1. Polymer matrix optimisation

To identify the effect of the polymer curing conditions (time and temperature) on the mechanical properties of the composites at room temperature and at the range of intended healing temperatures (70-100°C), Figure 2 shows the storage modulus-temperature relation for different curing conditions. At each temperature, the glass transition temperature (T_g) and the storage modulus (E') increase with the curing temperature and time. The increase in E' is most remarkable when $T>T_g$ which indicates an increase in the crosslinking density.

The general stress-strain relations of the polymer matrix after different curing conditions are given in Supplementary Information S1. Derived from these results, Figure 3 shows the variation of the Young's modulus of the polymer matrix after different curing conditions. It is shown that a combination of adequate curing time and temperature leads to a room temperature stiffness higher than 1000 MPa, which is in the same order of magnitude as that of commercial epoxy matrices. These experiments show that the elastic modulus of the modified matrix after the selected curing treatment is reaching the lower limits of the target region for intrinsic self-healing polymers depicted in Figure 1.

Self-healing polymer matrices to be used for structural composites require a modulus that is high at room/service temperature and relatively low at the targeted healing temperatures so the matrix obtains sufficient mobility to heal while retaining its structural integrity [45]. From Figure 2 and Figure 3 it can be extracted that this combination of properties can be best achieved with a curing process at 100°C for 60 hours amongst all the curing conditions evaluated in this study. Therefore these curing conditions are used troughout the remainder of this study. However, it has to be noted

that a more extensive study on these characteristics will most likely lead to a further optimized set of curing parameters.

3.2. Composite characterization

Using the curing conditions derived in section 3.1, GFRP laminates were prepared by conventional vacuum infusion processing. As a result, composites with a fibre volume fraction of 51.0 ± 0.9% were obtained (assuming a negligible porosity). Consecutively, the flexural, interlaminar fracture and impact properties were tested before and after healing with 3-point bending, DCB and low-velocity impact testing respectively.

3.2.1. Flexural properties

Figure 4 shows the flexural stress-strain relation for different composite beams after multiple healing treatments (always for 16 hours at 0.2 bar) at different healing temperatures. From the curves of the pristine specimen an average flexural modulus of 10.1±0.7 GPa and yield strength of 55.0±3.7 MPa can be derived. These values are approaching those of high-performance composites, although they are not yet at a level where they can fully compete with these materials on a commercial level [23].

The results in Figure 4 show that after the first healing treatment, the level of repair depends on the selected healing temperature and that the highest healing temperature (100°C) leads to the highest levels of flexural modulus and yield strength recovery. The development of these mechanical properties is more clearly depicted in Figure 5, which reports the 0.1% offset yield strength and flexural modulus versus the number of bending cycles. Figure 5 also shows that the flexural modulus slightly increases after the first healing cycle for all healing temperatures applied. This is attributed to the post-curing of the unreacted alkoxysilane groups. The theory that the post-curing effect is the main explanation for the healing observed is discarded by dedicated further testing as is shown in Supplementary Information S2.

When multiple healing is taken into account, it is observed that the yield strength slowly decreases as the number of healing treatments is increased. However, for a multiple healing treatment of 100°C, the yield strength drops much faster compared to the other healing temperatures. At the fourth bending cycle the resulting yield strength is almost at the level of the non-temperature treated reference specimen, indicating that the healing potential is almost depleted. These results therefore show that for an application with a yield strength design limit of 30 MPa it is better to use a temperature of 85°C as a longer lifetime extension is obtained. A similar trend seems to be present for the calculated flexural modulus although the decay of this property (at a healing temperature of 100°C) sets in later than that of the yield strength. The loss of healing efficiency over time is most likely caused by the slow oxidation of thiol groups which are known to assist the healing via reversible disulfide chemistry [49]. This thiol oxidation is faster when a higher temperature is applied [28]. As a result, the healing potential of these composites is not inexaustable when low healing pressures are applied. Since healing at 85°C is seemingly most optimal, this temperature is selected as the healing temperature for the other composite healing experiments in the rest of the study.

Another interesting feature observed in Figure 4 is that after healing, the stress value at high strain levels is higher than that of a pristine specimen. As it turns out, the modulus at high strain (> 1.0%) of the healed composites is equal to that of the pristine matrix (Supplementary Information S3). At these strain levels it is therefore probable that the stress response is dominated by the polymer matrix which after healing compensates for the broken glass fibres. The flow of the matrix towards the cracks during healing is further illustrated by the OM images in Figure 6, which show the cracked regions of the composite before and after healing. The micrographs confirm that the matrix material slightly flows upon a healing treatment, thereby partially filling the crack volume.

3.2.2. Interlaminar fracture properties

To investigate the recovery of the interlaminar fracture properties, the composites were tested in Mode I DCB. In doing so, delaminated areas of 10-15 cm^2 were created. Such damage areas are several orders of magnitude larger than the μm^2-mm^2 damage areas generated in the flexural tests. It was observed that the pressure applied during healing has a profound effect on such macroscale damage and therefore this effect was investigated in more detail by applying healing pressures of 0.2, 2 and 20 bar. Figure 7 shows the load-displacement curves of a fractured composite beam healed at 2 bar (for 16 hours at 85°C) for multiple healing cycles. In addition, the crack development during the experiment is shown. The force-displacement curves for the other applied healing pressures are shown in Supplementary Information S5.

From Figure 7 it can be observed that after the 1st healing treatment, upon reloading, the crack at the healed region propagates faster and that the measured maximum force is somewhat lower than that for the pristine specimen, indicating only partial damage healing. Upon the application of multiple healing cycles, the onset of crack propagation starts at an increasingly earlier stage for each damage and healing cycle. Still, the rate of crack propagation and the force development are similar for each healing cycle, which indicates that successful multiple healing is obtained.

Figure 8 further explores the effect of healing pressure on the fracture toughness healing by showing the calculated interlaminar fracture toughness (G_I) versus the normalized crack length. From this figure it is observed that the composites have a lower initial fracture toughness than that of commercially available epoxy based thermosets (>1000 kJ/m^2) [23], which is in line with the comparison of the other identified mechanical properties and results obtained in previous work that describe a decrease in G_I as the ultimate strength of an epoxy based matrix is lowered [21,23]. Furthermore Figure 8 more clearly describes the partial healing observed in Figure 7 as the fracture toughness after each healing cycle does not reach the G_I values of the pristine specimen. It is observed that a minimal pressure of 0.2 bar leads to a low level of fracture toughness recovery and that this level almost drops to zero when multiple healing treatments are applied (the small increase in G_I near the end of the propagated crack does not correspond to healing, but is caused

by resistance build-up at the non-propagated zone). More interestingly, an applied pressure of 20 bar leads to a near complete recovery of G_I after each applied healing cycle. This indicates that full healing of the fracture toughness can be obtained as long as the damaged interfaces are brought into adequate contact. The interface mismatch will naturally be higher for the large scale delaminations created by Mode I opening compared to the μm^2-mm^2 scale damage caused by flexural tests. Hence, the requirement for a higher external healing pressure can be explained.

It has to be noted that it is disputable whether the application of high pressure heat treatments (>10 bar) is technologically very relevant since applying such pressures on-site on larger actual composite structures introduces obvious practical problems. However, as smaller de-mounted composite components can still be repaired more easily than with the conventional thermoset repair routes, the proposed strategy is still beneficial to extend the lifetime of composite products. These results also indicate that the focus of composite healing relevant to real applications for the time being should be on the recovery of early stage damage with minimal crack opening (or automated crack closure) as healing in this case can be performed at moderate temperatures and pressures.

3.2.3. Low-velocity impact properties

Impact damage is one of the most frequently occurring damage modes in FRCPs. Therefore, the healing of low-velocity impact was selected as the final composite characterization technique in this study. Figure 9 shows an example of the image analysis on the healing (16 hours, 85°C, 0.2 bar) of low-velocity impact damage for 3 different levels of impact energy.

The first set of impact studies focussed on an impact energy of 30 J in accordance with ASTM D7136. Figure 9 indicates that an impact of 30 J results in a large portion of fibre breakage and consequently only a small reduction of damaged area after healing is observed. Since only damage in the polymer phase can be healed, two additional sets of impact experiments at lower energies (16J and 8J) were performed in which the relative amount of matrix damage versus fibre

failure would be higher. Firstly, it is found that the calculated dissipated energy is more than half of the induced energy for all impact conditions. This is an interesting feature for applications that require high damping properties. It was found that the level of dissipated energy did nog change significantly after the initial damage or healing treatment (Supplementary Information S6). Secondly, Figure 9 shows that as impact energy decreases the amount of visual damage is reduced, but more importantly that the area reduction due to healing increases. This trend is visualized more clearly in Figure 10, which shows the percentage of damage area reduction versus the applied impact energy. From this figure a near-linear trend emerges which indicates that only small impact events can be fully healed and that attempts on healing heavy impact event (>30 J energy) will be futile for the current system at a healing pressure of 0.2 bar.

4. Conclusion

Using a novel epoxy-based thermoset matrix, a GFRP composite with the ability to restore mechanical properties upon a low temperature treatment was developed. This composite has a currently unchallenged combination of a decent stiffness (800-1200 MPa), moderate healing temperatures (70-85°C) below the curing temperature, good damping properties, and the possibility to process by conventional vacuum infusion. Mechanical characterization of the composites demonstrated multiple healing of flexural and interlaminar fracture properties. Additionally the healing of low-energy impact damage was demonstrated. It was found that only minimal pressure is required for the healing of small scale ($<cm^2$) sized damage. For large scale damage ($>cm^2$) more healing pressure is required to perfectly align the damaged interfaces and bring back crack faces into contact. However, with high healing pressures full recovery after multiple healing cycles can be obtained provided the damage is concentrated in the matrix phase. Overall, this study shows a self-healing GFRP with mechanical properties that are adequate for medium-tech applications and opens the path towards the development of intrinsic low-temperature self-healing composites with high-end applications.

Acknowledgements

The authors gratefully acknowledge funding from European Union's Seventh Framework Programme under grant agreement number 314768 and the Swiss National Science Foundation (SNF 200020-150007-1).

References

1. Pang, J.W.C.; Bond, I.P. A hollow fibre reinforced polymer composite encompassing self-healing and enhanced damage visibility. *Composites Science and Technology* **2005**, *65*, 1791-1799.
2. Williams, H.R.; Trask, R.S.; Bond, I.P. Self-healing sandwich panels: Restoration of compressive strength after impact. *Composites Science and Technology* **2008**, *68*, 3171-3177.
3. Toohey, K.S.; Sottos, N.R.; Lewis, J.A.; Moore, J.S.; White, S.R. Self-healing materials with microvascular networks. *Nature Materials* **2007**, *6*, 581-585.
4. García, S.J. Effect of polymer architecture on the intrinsic self-healing character of polymers. *European Polymer Journal* **2014**, *53*, 118-125.
5. Blaiszik, B.J.; Kramer, S.L.B.; Olugebefola, S.C.; Moore, J.S.; Sottos, N.R.; White, S.R. Self-healing polymers and composites. In *Annual Review of Materials Research*, 2010; Vol. 40, pp 179-211.
6. Neuser, S.; Chen, P.W.; Studart, A.R.; Michaud, V. Fracture toughness healing in epoxy containing both epoxy and amine loaded capsules. *Advanced Engineering Materials* **2014**, *16*, 581-587.
7. Trask, R.S.; Williams, G.J.; Bond, I.P. Bioinspired self-healing of advanced composite structures using hollow glass fibres. *Journal of the Royal Society Interface* **2007**, *4*, 363-371.
8. Prajer, M.; Wu, X.; García, S.J.; van der Zwaag, S. Direct and indirect observation of multiple local healing events in successively loaded fibre reinforced polymer model composites using healing agent-filled compartmented fibres. *Composites Science and Technology* **2015**, *106*, 127-133.
9. Manfredi, E.; Cohades, A.; Richard, I.; Michaud, V. Assessment of solvent capsule-based healing for woven e-glass fibre-reinforced polymers. *Smart Materials and Structures* **2015**, *24*.
10. Brown, E.N.; Sottos, N.R.; White, S.R. Fracture testing of a self-healing polymer composite. *Experimental Mechanics* **2002**, *42*, 372-379.
11. Trask, R.S.; Bond, I.P. Biomimetic self-healing of advanced composite structures using hollow glass fibres. *Smart Materials and Structures* **2006**, *15*, 704-710.
12. Williams, G.J.; Bond, I.P.; Trask, R.S. Compression after impact assessment of self-healing cfrp. *Composites Part A: Applied Science and Manufacturing* **2009**, *40*, 1399-1406.
13. Zhong, N.; Post, W. Self-repair of structural and functional composites with intrinsically self-healing polymer matrices: A review. *Composites Part A: Applied Science and Manufacturing* **2015**, *69*, 226-239.
14. Coope, T.S.; Turkenburg, D.H.; Fischer, H.R.; Luterbacher, R.; Van Bracht, H.; Bond, I.P. Novel diels-alder based self-healing epoxies for aerospace composites. *Smart Materials and Structures* **2016**, *25*.
15. Peterson, A.M.; Jensen, R.E.; Palmese, G.R. Room-temperature healing of a thermosetting polymer using the diels-alder reaction. *ACS Applied Materials and Interfaces* **2010**, *2*, 1141-1149.

16. Peterson, A.M.; Jensen, R.E.; Palmese, G.R. Kinetic considerations for strength recovery at the fiber-matrix interface based on the diels-alder reaction. *ACS Applied Materials and Interfaces* **2013**, *5*, 815-821.
17. Bose, R.K.; Hohlbein, N.; García, S.J.; Schmidt, A.M.; van der Zwaag, S. Connecting supramolecular bond lifetime and network mobility for scratch healing in poly(butyl acrylate) ionomers containing sodium, zinc and cobalt. *Physical Chemistry Chemical Physics* **2015**, *17*, 1697-1704.
18. Wang, C.H.; Sidhu, K.; Yang, T.; Zhang, J.; Shanks, R. Interlayer self-healing and toughening of carbon fibre/epoxy composites using copolymer films. *Composites Part A: Applied Science and Manufacturing* **2012**, *43*, 512-518.
19. Post, W.; Bose, R.; García, S.; van der Zwaag, S. Healing of early stage fatigue damage in ionomer/fe3o4 nanoparticle composites. *Polymers* **2016**, *8*, 436.
20. Sordo, F.; Michaud, V. Processing and damage recovery of intrinsic self-healing glass fiber reinforced composites. *Smart Materials and Structures* **2016**, *25*.
21. Cohades, A.; Manfredi, E.; Plummer, C.J.G.; Michaud, V. Thermal mending in immiscible poly(ϵ-caprolactone)/epoxy blends. *European Polymer Journal* **2016**, *81*, 114-128.
22. Luo, X.; Ou, R.; Eberly, D.E.; Singhal, A.; Viratyaporn, W.; Mather, P.T. A thermoplastic/thermoset blend exhibiting thermal mending and reversible adhesion. *ACS Applied Materials and Interfaces* **2009**, *1*, 612-620.
23. Cohades, A.; Michaud, V. Thermal mending in e-glass reinforced poly(ε-caprolactone)/epoxy blends. *Composites Part A: Applied Science and Manufacturing* **2017**, *99*, 129-138.
24. Sastri, V.R.; Tesoro, G.C. Reversible crosslinking in epoxy resins. Ii. New approaches. *Journal of Applied Polymer Science* **1990**, *39*, 1439-1457.
25. Tesoro, G.C.; Sastri, V. Reversible crosslinking in epoxy resins. I. Feasibility studies. *Journal of Applied Polymer Science* **1990**, *39*, 1425-1437.
26. Canadell, J.; Goossens, H.; Klumperman, B. Self-healing materials based on disulfide links. *Macromolecules* **2011**, *44*, 2536-2541.
27. Abdolah Zadeh, M.; van der Zwaag, S.; García, S.J. Self-healing corrosion-protective sol-gel coatings based on extrinsic and intrinsic healing approaches. In *Advances in Polymer Science*, 2016; Vol. 273, pp 185-218.
28. Abdolahzadeh, M.; C. Esteves, A.C.; van der Zwaag, S.; García, S.J. Healable dual organic-inorganic crosslinked sol-gel based polymers: Crosslinking density and tetrasulfide content effect. *Journal of Polymer Science, Part A: Polymer Chemistry* **2014**, *52*, 1953-1961.
29. Hernández, M.; Grande, A.M.; Dierkes, W.; Bijleveld, J.; van der Zwaag, S.; García, S.J. Turning vulcanized natural rubber into a self-healing polymer: Effect of the disulfide/polysulfide ratio. *ACS Sustainable Chemistry and Engineering* **2016**, *4*, 5776-5784.
30. Zhong, N.; García, S.J.; van der Zwaag, S. The effect of filler parameters on the healing of thermal conductivity and mechanical properties of a thermal interface material based on a self-healable organic-inorganic polymer matrix. *Smart Materials and Structures* **2016**, *25*.
31. Ruiz de Luzuriaga, A.; Martin, R.; Markaide, N.; Rekondo, A.; Cabanero, G.; Rodriguez, J.; Odriozola, I. Epoxy resin with exchangeable disulfide crosslinks to obtain reprocessable, repairable and recyclable fiber-reinforced thermoset composites. *Materials Horizons* **2016**, *3*, 241-247.
32. Susa, A.; Bose, R.K.; Grande, A.M.; van der Zwaag, S.; García, S.J. Effect of the dianhydride/branched diamine ratio on the architecture and room temperature healing behavior of polyetherimides. *ACS Applied Materials and Interfaces* **2016**, *8*, 34068-34079.
33. Chen, Y.; Kushner, A.M.; Williams, G.A.; Guan, Z. Multiphase design of autonomic self-healing thermoplastic elastomers. *Nat Chem* **2012**, *4*, 467-472.
34. Montarnal, D.; Cordier, P.; Soulié-Ziakovic, C.; Tournilhac, F.; Leibler, L. Synthesis of self-healing supramolecular rubbers from fatty acid derivatives, diethylene triamine, and urea. *Journal of Polymer Science Part A: Polymer Chemistry* **2008**, *46*, 7925-7936.

35. Montarnal, D.; Tournilhac, F.; Hidalgo, M.; Couturier, J.-L.; Leibler, L. Versatile one-pot synthesis of supramolecular plastics and self-healing rubbers. *Journal of the American Chemical Society* **2009**, *131*, 7966-7967.
36. Sordo, F.; Mougnier, S.J.; Loureiro, N.; Tournilhac, F.; Michaud, V. Design of self-healing supramolecular rubbers with a tunable number of chemical cross-links. *Macromolecules* **2015**, *48*, 4394-4402.
37. Agache , P.G.; Monneur, C.; Leveque, J.L.; De Rigal, J. Mechanical properties and young's modulus of human skin in vivo *Archives of Dermatological Research* **1980**, *269*, 221-232.
38. Bode, S.; Bose, R.K.; Matthes, S.; Ehrhardt, M.; Seifert, A.; Schacher, F.H.; Paulus, R.M.; Stumpf, S.; Sandmann, B.; Vitz, J.*, et al.* Self-healing metallopolymers based on cadmium bis(terpyridine) complex containing polymer networks. *Polymer Chemistry* **2013**, *4*, 4966-4973.
39. Rahman, M.A.; Spagnoli, G.; Grande, A.M.; Di Landro, L. Role of phase morphology on the damage initiated self-healing behavior of ionomer blends. *Macromolecular Materials and Engineering* **2013**, *298*, 1350-1364.
40. Dello Iacono, S.; Martone, A.; Filippone, G.; Acierno, D.; Zarrelli, M.; Giordano, M.; Amendola, E. In *Insight on mendable resin made by combining diels-alder epoxy adducts with dgeba*, AIP Conference Proceedings, 2016.
41. Bose, R.K.; Kötteritzsch, J.; García, S.J.; Hager, M.D.; Schubert, U.S.; van der Zwaag, S. A rheological and spectroscopic study on the kinetics of self-healing in a single-component diels–alder copolymer and its underlying chemical reaction. *Journal of Polymer Science Part A: Polymer Chemistry* **2014**, *52*, 1669-1675.
42. Montarnal, D.; Capelot, M.; Tournilhac, F.; Leibler, L. Silica-like malleable materials from permanent organic networks. *Science* **2011**, *334*, 965-968.
43. Röttger, M.; Domenech, T.; van der Weegen, R.; Breuillac, A.; Nicolaÿ, R.; Leibler, L. High-performance vitrimers from commodity thermoplastics through dioxaborolane metathesis. *Science* **2017**, *356*, 62-65.
44. NETZSCH. Thermal properties of polymers. NETZSCH, Ed. 2016.
45. Abdolah Zadeh, M.; Grande, A.M.; van der Zwaag, S.; García, S.J. Effect of curing on the mechanical and healing behaviour of a hybrid dual network: A time resolved evaluation. *RSC Advances* **2016**, *6*, 91806-91814.
46. Standard test method for flexural properties of unreinforced and reinforced plastics and electrical insulating materials by four-point bending. ASTM International: 2017.
47. Standard test method for mode i interlaminar fracture toughness of unidirectional fiber-reinforced polymer matrix composites. ASTM International: 2013.
48. Standard test method for measuring the damage resistance of a fiber-reinforced polymer matrix composite to a drop-weight impact event. ASTM International: 2015.
49. Pepels, M.; Filot, I.; Klumperman, B.; Goossens, H. Self-healing systems based on disulfide-thiol exchange reactions. *Polymer Chemistry* **2013**, *4*, 4955-4965.

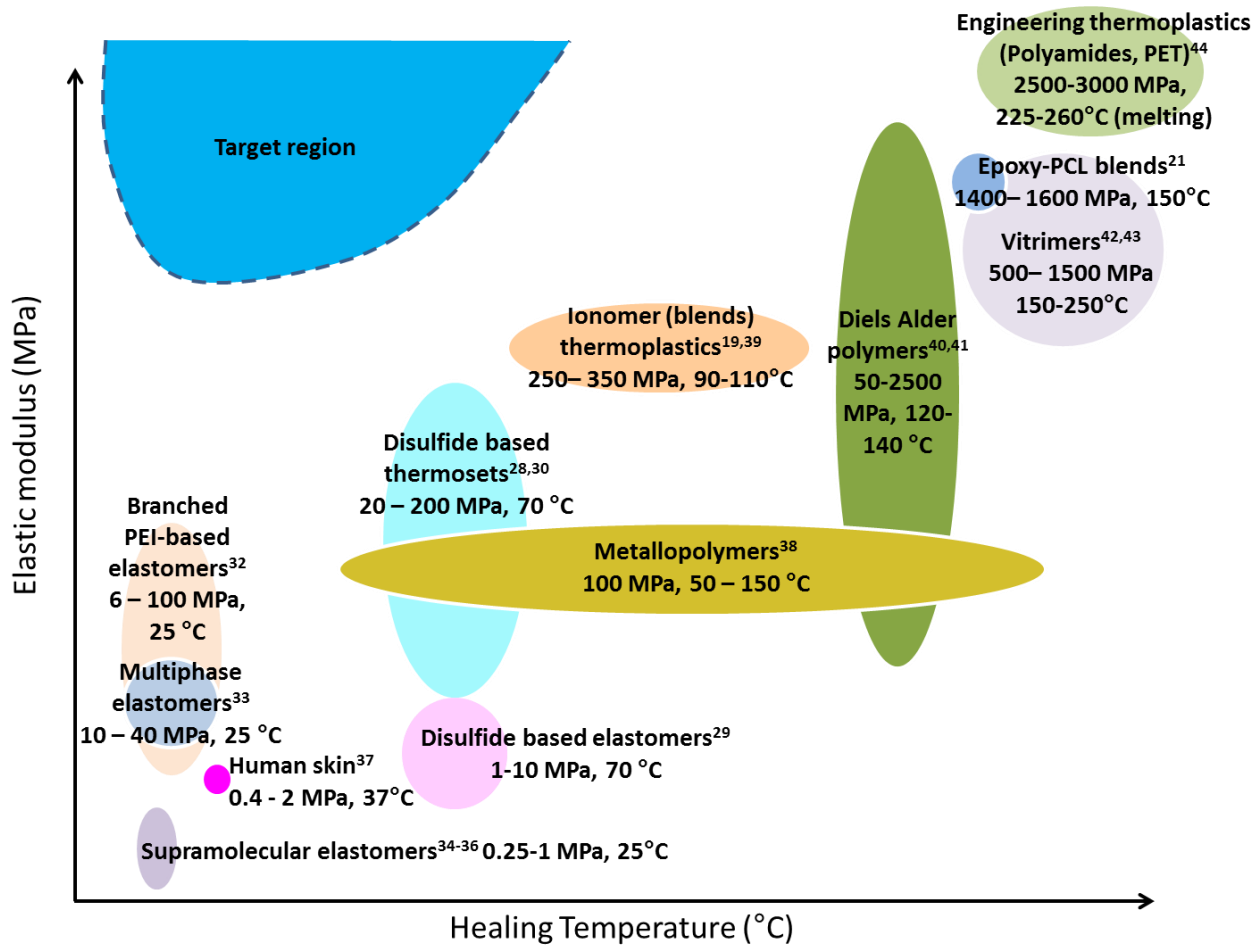

Figure 1 Overview of elastic modulus versus healing temperature of a wide range of intrinsic self-healing polymer matrices developed in the past decade.

Table I Weight ratio of resin components in the self-healing polymer matrix

Resin component	Weight ratio
Epon ™ 828	1
Ancamine®2500	0,646
(3-Aminopropyl)trimethoxysilane	0,076
Pentaerythritol tetrakis(3-mercaptopropionate)	0,579
Bis[3-(triethoxysilyl)propyl]disulfide	0,566
Triethylamine	0,014

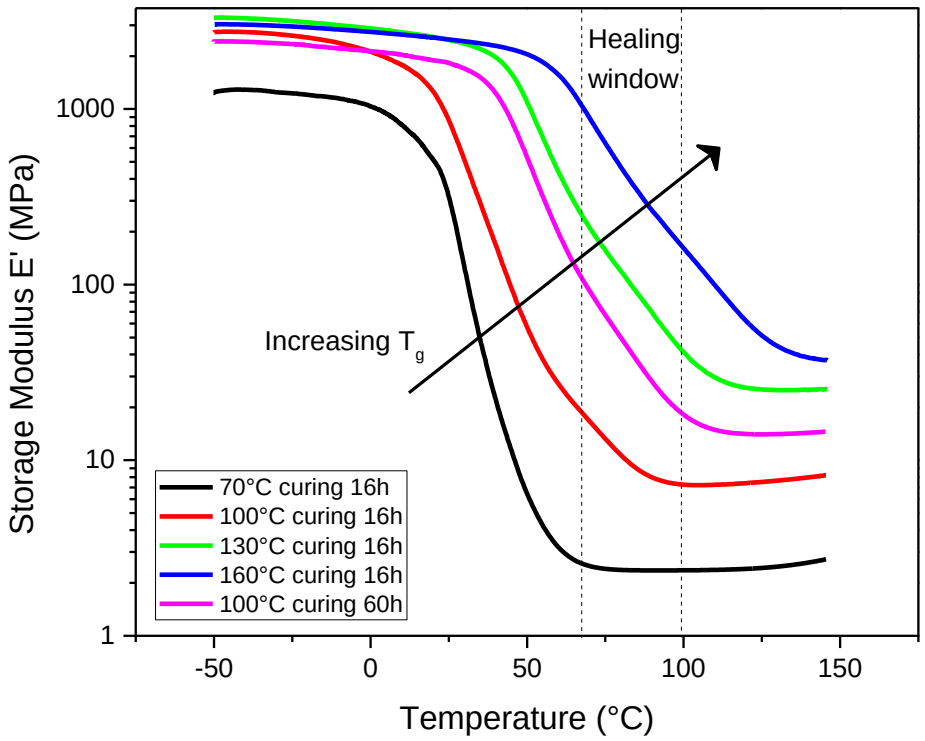

Figure 2 Storage modulus vs. temperature of the dual network polymer matrix after different curing conditions.

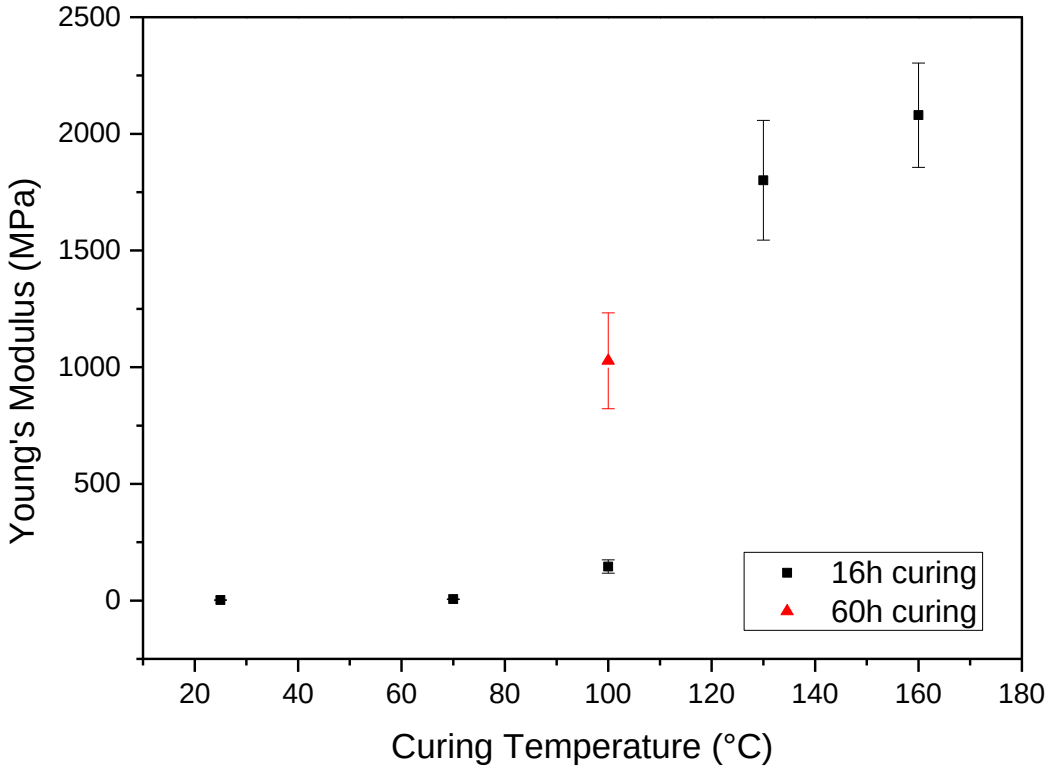

Figure 3 Effect of the curing treatment on the resulting tensile stiffness of the dual network polymer matrix

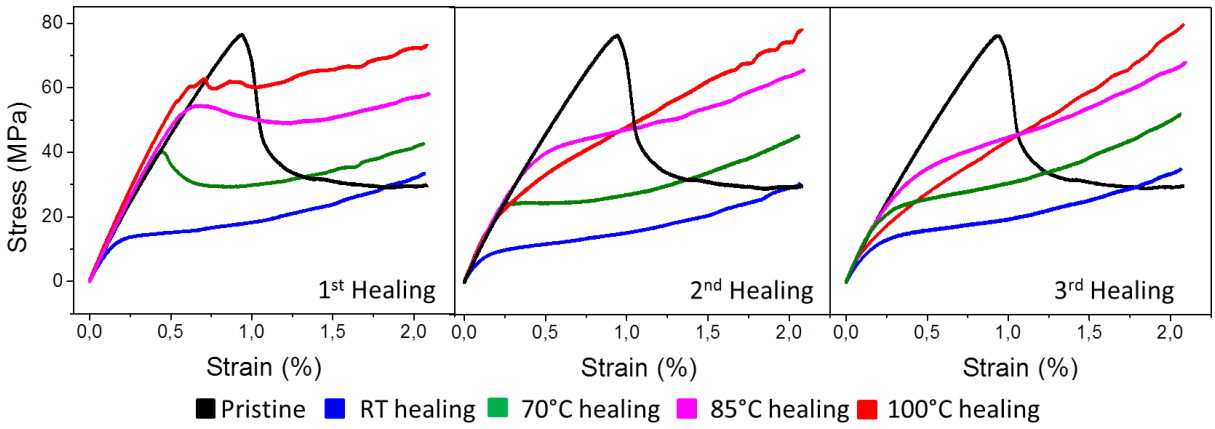

Figure 4 Stress-strain curves of the flexural tests performed on composite beams. The figure shows the flexural properties of 3 consecutive runs of healing treatments for 4 different healing temperatures compared to a pristine test. Specimen were healed for 16 hours at a moderate pressure of 0.2 bar.

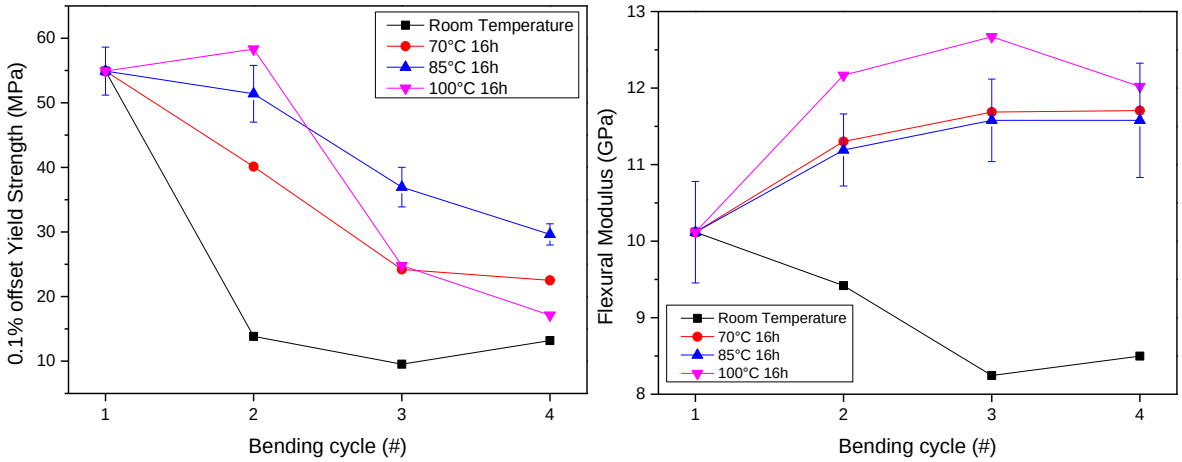

Figure 5 Effect of the selected healing temperature on the multiple healing of the yield strength and the stiffness. Healing is performed for 16 hours at 0.2 bar at different temperatures (70, 85 and 100 °C).

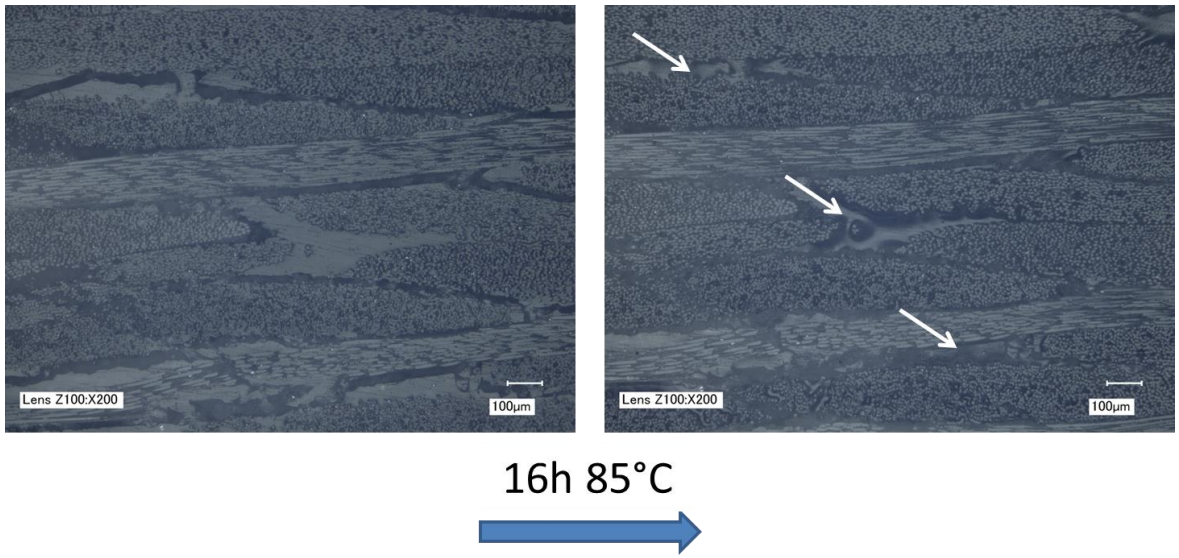

Figure 6 Optical microscopy images of a composite that has been subjected to 3-point bending before (left) and after (right) healing. Images are taken perpendicular (z-direction) of the bending direction. White arrows indicate regions of visible matrix flow.

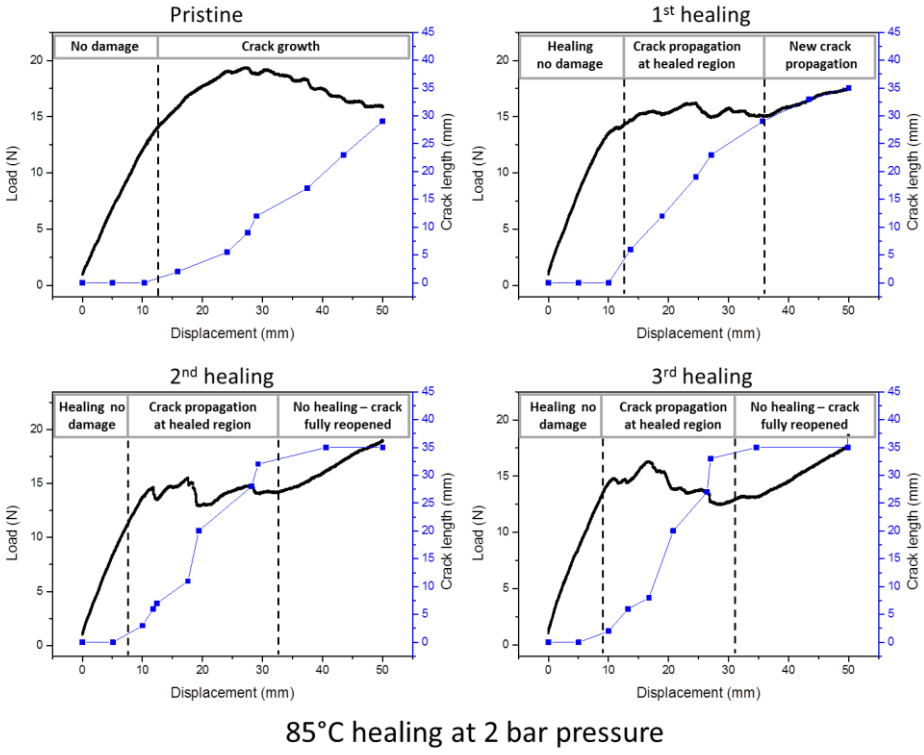

Figure 7 Combined load-displacement/crack propagation curves of the Mode I opening of a composite healed three times at 85°C and 2 bar pressure for 16 hours.

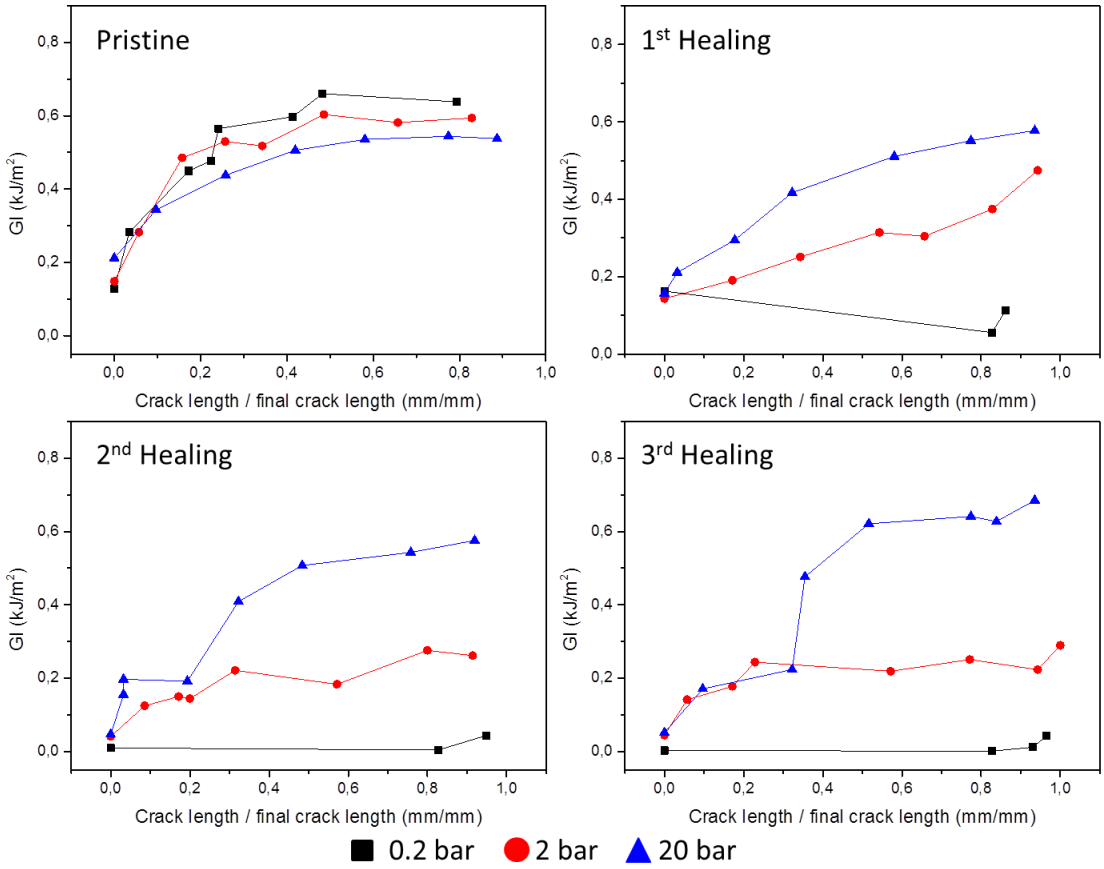

Figure 8 Interlaminar fracture toughness plotted versus the normalized crack growth in Mode I opening for 3 consecutive healing treatments at different pressures. Healing is performed at 85°C for 16 hours.

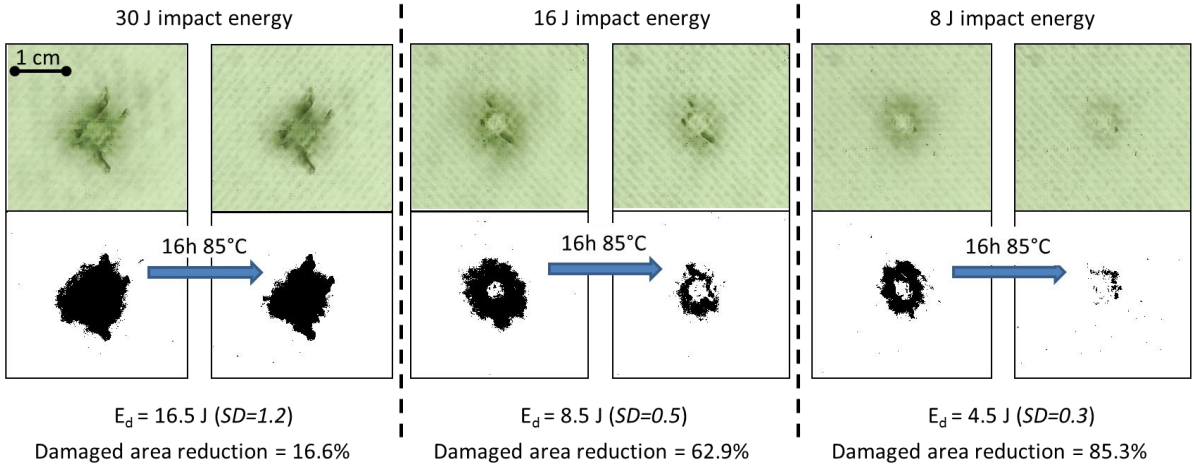

Figure 9 Image analysis of the healing of low-velocity impact for 3 different levels of impact energy. Healing is performed at 85°C and 0.2 bar for 16 hours. Top images show the real damaged composite whereas the bottom pictures show the same pictures treated with a binary filter to facilitate the characterization.

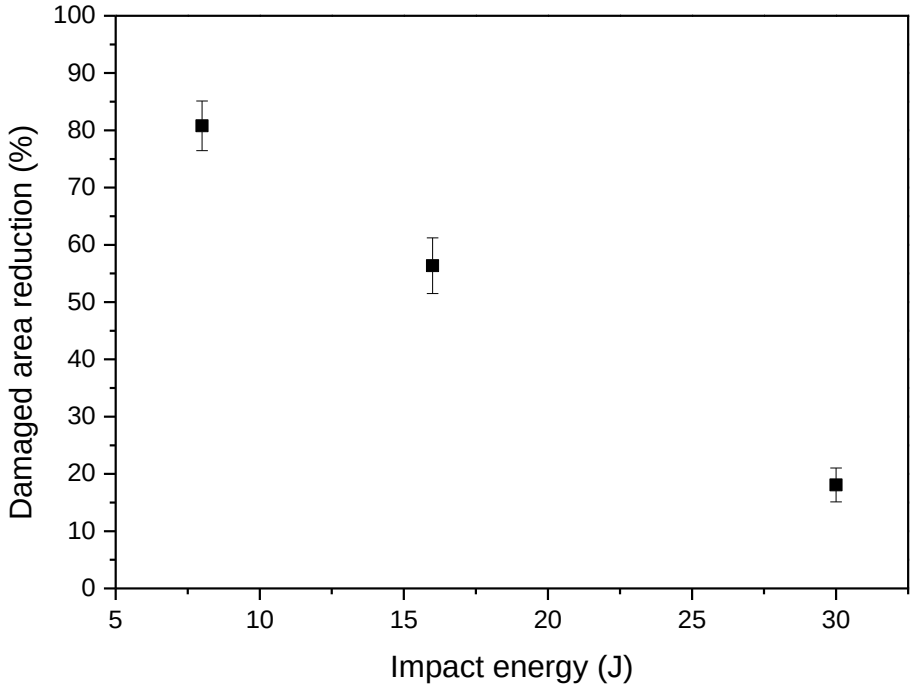

Figure 10 Damaged area reduction plotted against the initial impact energy.